

NEW METHOD FOR MODELING THE POLLUTANT DISPERSION IN CONVECTIVE ATMOSPHERIC BOUNDARY LAYER

Boris B. Ilyushin

Institute of Thermophysics, Novosibirsk, Russia
ilyushin@itp.nsc.ru

ABSTRACT

Experimental and theoretical investigations confirm the formation of Coherent Large Scale Eddy Structure (CS) in convective atmospheric boundary layer (ABL). They contain the main part of the turbulence energy and the turbulent transfer is achieved mainly by the action of CS. Such non-local turbulent transfer cannot be described within "standard" turbulent diffusion models of gradient type. The turbulent transport models of third- and second- order closure are presented in the paper (Ilyushin and Kurbatskii, 1997). These models describe the statistic structure of convective ABL adequately of the experimental data. In this paper the results of modeling of the pollutant turbulent transfer in ABL are presented. The approach based on accounting the influence of the CS by accentuation of the periodic properties of motions, which is analogous to VLES is used. But in this paper the accentuation of periodic motions are obtained for the pdf of vertical velocity field.

PDF RECONSTRUCT FOR CONVECTIVE ATMOSPHERIC BOUNDARY LAYER.

Convective atmospheric boundary layer is usually taken to mean the atmospheric layer where there is a direct influence from the underlying surface heated by the sunrays. For conditions where the Rayleigh number in the lower regions of ABL becomes larger than some critical value, large-

eddy convective motions similar to Benard cells appear and play a main role in the vertical transfer of momentum, heat and substance. Circulation in such cells is shown schematically in Fig.1b at the plane XZ. Non-symmetric boundary conditions (heating below, stable stratification at the upper boundary) cause an asymmetric distribution of the PBL vertical velocity amplitudes: steep rising motions and gentler descending ones (see Fig.1a). Such a character of the motion has been confirmed by field experiments (Byzova et al., 1991). The curve in Fig.1c represents a typical realization of the vertical component of velocity for unstable stratification obtained at an altitude of 120 m and smoothed over a period of about one minute. This curve is not exactly periodic because it represents a cross-section of a quasi-regular system of cells. However, noting the character of this curve, one can recognize that such a realization corresponds to the velocity field along a line passing through the cells centers. The horizontal size of the cells λ is between three and five kilometers. The cells occupy in the vertical direction practically the whole ABL, the distributions of statistical characteristics of the velocity and temperature fields (second- and third-order moments) reflected such structure of the convective ABL have been calculated by Ilyushin (1998) and are shown in Fig.2 together with the data of measurements in the convective ABL taken from (Caughy, 1982) and (Lenschow et al., 1980). One can see that calculated profiles are in good agreement with the data of observations and can be used to reconstruct the pdf of the vertical velocity fluctuation in the convective ABL.

The pdf of the turbulent fluctuations of the vertical velocity is represented as a superposition of two independent distributions: the inertial range of the turbulent spectrum (background turbulence) $P_b(u)$ and a large-wave region pdf spectrum $P_c(v)$ (u and v are the vertical velocity fluctuations of background turbulence and the vertical velocity field of coherent structures, correspondingly)

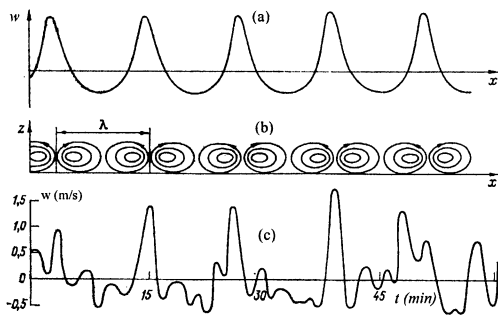


Figure 1. Vertical motion shape in the convective Large scale eddies (a,b) and the measured realization of vertical velocity smoothed with the period 1 min. (c).

$$P(u,v) = P_b(u)P_c(v) = \underbrace{\frac{1}{2\pi\sigma_b} \exp\left\{-\frac{u^2}{2\sigma_b^2}\right\}}_{\text{background turbulence PDF}} \times$$

$$\underbrace{\left[\frac{a^+}{\sigma_c^+} \exp\left\{-\frac{(m^+ - v)^2}{2(\sigma_c^+)^2}\right\} + \frac{a^-}{\sigma_c^-} \exp\left\{-\frac{(m^- - v)^2}{2(\sigma_c^-)^2}\right\} \right]}_{\text{Large Scale Eddy Formation PDF}} \quad (1)$$

where σ_b is the dispersion of background turbulence; a^+ and a^- are weighting coefficients, σ_c^+ and σ_c^- are the dispersions, m^+ and m^- are the distribution maximums (the average velocities) of upflow and downflow of coherent structures. Considering the total turbulent velocity fluctuation w as the sum of u and v , we obtain the total pdf:

$$P(w) = \int_R P(u, v) \delta(w - u - v) du dv = \frac{a^+}{2\pi\sigma_+} \exp\left\{-\frac{(m^+ - w)^2}{2\sigma_+^2}\right\} + \frac{a^-}{2\pi\sigma_-} \exp\left\{-\frac{(m^- - w)^2}{2\sigma_-^2}\right\} \quad (2)$$

where $\sigma_+^2 = (\sigma_c^+)^2 + \sigma_b^2$, $\sigma_-^2 = (\sigma_c^-)^2 + \sigma_b^2$. From the conditions

$$\int_R P(w) dw = 1 \quad \int_R wP(w) dw = 0$$

$$\int_R w^2 P(w) dw = \langle w^2 \rangle \quad \int_R w^3 P(w) dw = S_w \sigma^3 \quad (3)$$

($\sigma = \langle w^2 \rangle^{1/2}$ is the dispersion and $S_w = \langle w^3 \rangle / \langle w^2 \rangle^{3/2}$ is the skewness factor) the connections for a^+ , a^- , σ_+^2 , σ_-^2 , m^+ and m^- are the following:

$$a^+ + a^- = 1 \quad a^+ m^+ + a^- m^- = 0$$

$$a^+ [(m^+)^2 + \sigma_+^2] + a^- [(m^-)^2 + \sigma_-^2] = \sigma^2 \quad (4)$$

$$a^+ [(m^+)^3 + 3m^+ \sigma_+^2] + a^- [(m^-)^3 + 3m^- \sigma_-^2] = S_w \sigma^3$$

The conditions for σ_+^2 and σ_-^2 are found from the assumption (De Baas et al., 1986) that the square of the dispersions σ_+^2 and σ_-^2 should be equal to the square of the average velocities of upflow and downflow $(m^+)^2$ and $(m^-)^2$ correspondingly:

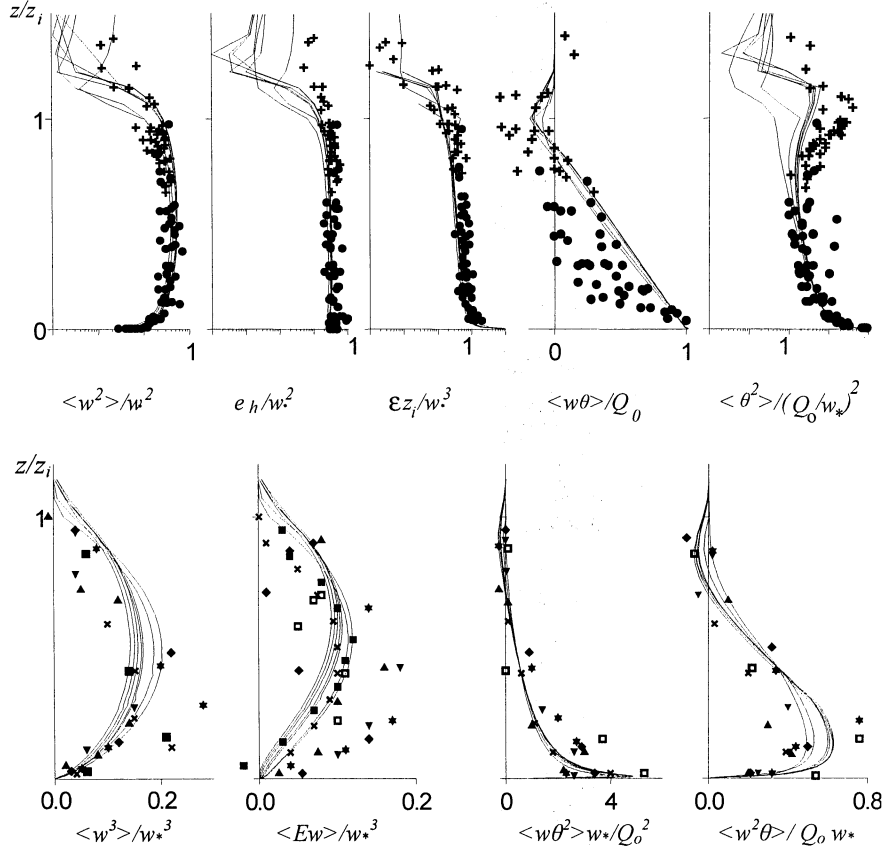


Figure 2. Results of simulation of the convective ABL evolution: solid lines are calculated profiles of second- and third-order correlations (different lines correspond to times from 10 a.m. to 5 p.m.); symbols are the experimental data.

$$\sigma_+^2 = (m^+)^2, \quad \sigma_-^2 = (m^-)^2 \quad (5)$$

This assumption means that flux directed positively (negatively) remains mainly positive (negative) taking into account possible scatter. The necessary conditions for closure of the equation set (for σ_b) is found from the wavelet model (Tennekes and Lumley, 1972). Here we suppose that the main part of the energy-containing range of the fluctuation spectrum is defined by a single main wavelet with a typical wave number corresponding to the spectrum maximum. The simplified eddy with a typical wave number κ_v is considered in the form of a localized perturbation of energy in wave number space (wavelet) with energy $E_v = E(\kappa_v) \kappa_v$. This consideration ensures the cascade transfer of turbulent energy from large-scale eddies to dissipative eddies. In the present work the coherent structure in the convective PBL is assumed to be the wavelet containing the energy $E_c = a\varepsilon^{2/3} \kappa_{max}^{-2/3}$ ($a = 1.6 \pm 0.02$ is the Kolmogoroff constant, κ_{max} is the maximum of the spectrum of the turbulent energy. The total turbulent energy can be calculate by integration of the inertial range (without accounting for the departure from the Kolmogoroff spectrum in the dissipation range) from κ_{max} to the infinity and with accounting also of the energy of half of the wavelet (which is outside of inertial range):

$$E \approx \int_{\kappa_{max}}^{\infty} a\varepsilon^{2/3} \kappa^{-5/3} d\kappa + \frac{1}{2} E_c = 2E_c \quad (6)$$

or $\sigma_b^2 = E$ ($(\sigma_b^2 + \sigma_c^2)/2 = E$). Accounting this result, κ_{max} is expressed as $\kappa_{max} = (2a/\varepsilon)^{3/2} \varepsilon$ and

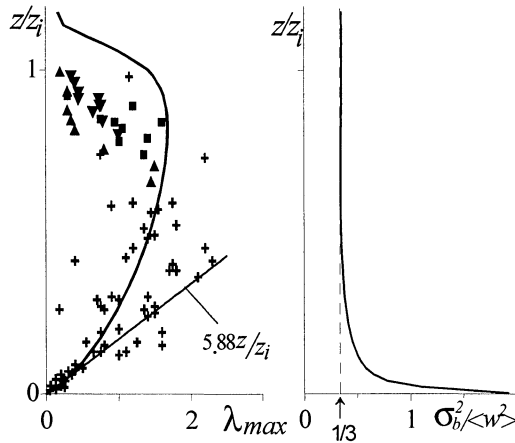


Figure 3. The calculated and measured (Caughey, 1982) profiles of $\lambda_{max} = 2\pi/\varepsilon (E/2a)^{3/2}$ and the ratio $\sigma_b^2 / \langle w^2 \rangle$.

then $\lambda_{max} = 2\pi/\kappa_{max}$. The calculated profiles of λ_{max} and the ratio $\sigma_b^2 / \langle w^2 \rangle$ in the convective atmosphere boundary layer are shown in Fig.3. Here one can see that in the mixing layer the calculated distribution of λ_{max} is in agreement with the observed data (Caughey, 1982). The linear function $\lambda_{max} = 5.88 z/z_i$ corresponds to conditions of free convection in the near-ground layer. The calculated ratio $\sigma_b^2 / \langle w^2 \rangle$ is equal to 1/3 in the mixing layer of the ABL. Analysis of the experimental spectrum of $\langle w^2 \rangle$ in the atmosphere (Monin and Yaglom, 1967) gives the same result $\sigma_b^2 / \langle w^2 \rangle \approx 1/3$. The necessary condition for the dispersion of the background turbulence σ_b is: $\sigma_b^2 = \frac{1}{3} \langle w^2 \rangle$. This equation and equations (4), (5) taking account of the variation in sign $m^+ > 0$ and $m^- < 0$ (which corresponds to upflow and downflow) have unique solutions:

$$\begin{aligned} m^+ &= \frac{\sigma}{4} \left[S + \sqrt{S^2 + 8} \right]; & m^- &= \frac{\sigma}{4} \left[S - \sqrt{S^2 + 8} \right]; \\ a^+ &= -\frac{S - \sqrt{S^2 + 8}}{2\sqrt{S^2 + 8}} & a^- &= \frac{S + \sqrt{S^2 + 8}}{2\sqrt{S^2 + 8}} \\ (\sigma_c^+)^2 &= \frac{\sigma^2}{16} \left[S + \sqrt{S^2 + 8} \right]^2 - \frac{1}{3} \langle w^2 \rangle & (7) \\ (\sigma_c^-)^2 &= \frac{\sigma^2}{16} \left[S - \sqrt{S^2 + 8} \right]^2 - \frac{1}{3} \langle w^2 \rangle \end{aligned}$$

The results of reconstructing the pdf using the calculated distributions of the second- and third-order moments are shown in Fig.4. The picture shows that the results of reconstruction correspond to the observed data: an upflow within a coherent structure with larger turbulent energy

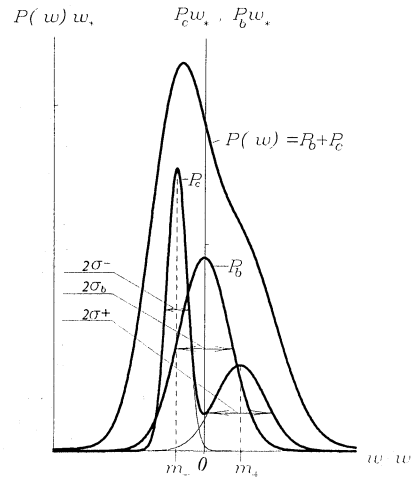


Figure 4. The reconstructed profile of pdf of the vertical velocity fluctuations for $z/z_i = 0.5$.

(σ_c^+) and larger velocity (m^+) occupying a smaller region (of size $\approx P_c(m^+) < P_c(m^-)$) and a downflow with smaller energy ($\sigma_c^- < \sigma_c^+$) and smaller velocity ($m^- < m^+$). Such a structure for the convective ABL arises from the vertical asymmetry in the generation mechanism for the turbulent fluctuations: in the near-ground layer a growth of turbulence energy is provided by the mean velocity shear whereas, in the upper (stably stratified) part of the ABL, turbulent fluctuations are strongly suppressed. Therefore the dispersion of the vertical velocity fluctuations in 'upflows' appears to be larger than that in 'downflows'. Figure 6 shows the pdf profiles obtained in the measurements (Byzova et al., 1991) in the atmosphere compared with calculations using the model of Deardorff. As is obvious the reconstructed pdf in the present work $P(w)$ (see Fig.4) is in qualitative agreement with those shown in Fig.5: it has the maximum in the region of negative velocities and the more convex part in that of positive velocities.

To obtain the distribution of vertical velocity fluctuations from individual realizations, it is necessary to apply a procedure of ensemble averaging. For horizontally homogeneous conditions, ensemble averaging and averaging over horizontal coordinates can be regarded as equivalent procedures. And finally, taking into account Taylor's hypothesis of frozen turbulence, averaging over horizontal coordinates can be replaced by time averaging for fixed horizontal

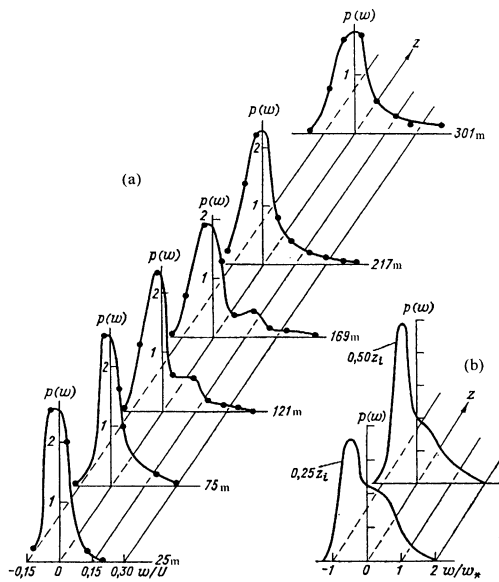


Figure 5. Distributions of vertical velocity variance in the convective ABL: (a) observed data and (b) calculation using the Deardorff's model (from (Byzova et al., 1991))

coordinates if the time of this averaging is larger than the drift (under the action of averaged flow) time D/U of the largest turbulent eddies. This allows us to decrease significantly the time required to obtain the measurements. Profiles of pdf shown in Fig.6 have been obtained using this method. The following assumptions have been used. For the horizontally homogeneous PBL the probability for the velocity to be within the range $[w; w + dw]$, $P(w)dw$ is proportional to a horizontal size of the region with such velocity $P(w)dw \sim dx$. The continuity condition of the velocity used for a region between large-scale eddies requires that the adjoining eddies have the opposite directions of swirling (see below fig. 6). The pair of such eddies we denote as a simple cell. For statistical analysis of the sequence of such identical cells carried by wind there is enough to study only one cell. This cell is represented as coherent structure which (within the adopted assumption) is a wavelet with the center in the location of κ_{max} and of the horizontal size λ_{max} . It is evident that the iterative character of the structures in the ABL makes the averaging within time interval $\lambda_{max}/(2U)$ and the averaging on infinite times interval to be equivalent. Thus, we may consider that the part of the reconstructed pdf having to do with coherent structures $P_c(w)$ as characterizing the local vertical fluxes up and down, that is one eddy (half of the cell). This allows us to reconstruct a single field of the vertical velocity (and then of the horizontal one) for this cell. As mentioned above, the size of the horizontal region of the coherent structures (where the vertical velocity is equal to \tilde{w}) is taken to be proportional to the probability $P_c(\tilde{w}) : P_c(\tilde{w})d\tilde{w} = dx/(\lambda_{max}/2)$. The vertical velocity field of the coherent structures $\tilde{w}(x, z)$ can be found from this differential equation. The horizontal velocity field $\tilde{u}(x, z)$ is determined from the equation of mass

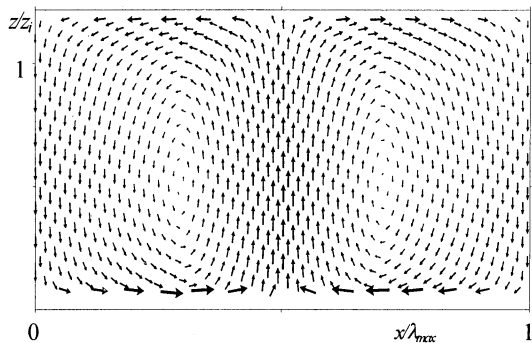


Figure 6. The reconstructed velocity field of the coherent structure in the convective PBL.

conservation. The result of reconstructing the coherent-structure velocity field (\tilde{u}, \tilde{w}) in the convective ABL is shown in Fig 6.

MODELING THE TURBULENT TRANSPORT OF SUBSTANCE

To describe the process of species dispersion in the convective ABL, we use a model taking directly into account the effect of mass transfer by coherent structures (in the advection terms of the equation for the crosswind integrated concentration). To account for the turbulent diffusion of matter by background turbulence, a "standard" gradient-diffusion model is applied:

$$\frac{\partial C_y}{\partial t} + (U + \tilde{u}) \frac{\partial C_y}{\partial x} + \tilde{w} \frac{\partial C_y}{\partial z} = \frac{\partial}{\partial z} \left[C_s \tau < w^2 > \frac{\partial C_y}{\partial z} \right] \quad (8)$$

where C_s is coefficient of the model. The value of C_s is determined from the condition that the coefficient of turbulent diffusion near the surface is approximated by $\kappa u_* z$ (Monin and Yaglom, 1967):

$$C_s \tau < w^2 > = \frac{2}{3} C_s \frac{E_0^2}{\epsilon_0} \approx 4.5^2 \frac{2}{3} C_s \kappa u_* z \Rightarrow C_s \approx 0.07$$

The results of a simulation of a pollutant jet spreading from sources placed both near ground level and in the middle of the mixed layer are presented. The crosswind integrated concentration fields averaged over one period, λ_{max}/U_{max} are

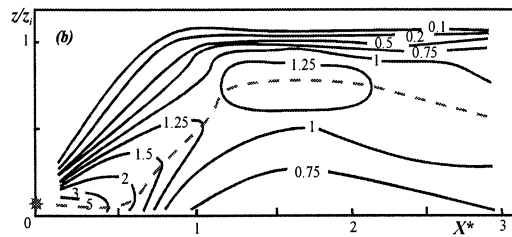
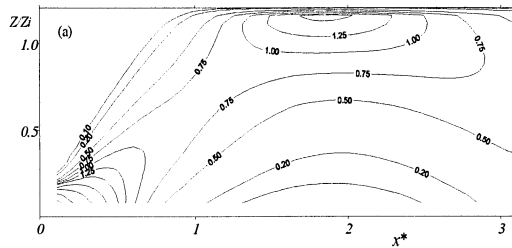


Figure 7. Calculated (a) and measured (Willis and Deardorff, 1976) (b) non-dimensional crosswind integrated concentration $C_y z_i U_x / q_0$ for point sources of height $z/z_i = 0.067$.

shown in figs. 7, 8. A near-ground source was realized at $z_s/z_i = 0.07$. The maximum concentration centerline (e.g., the locus of maximum concentration) first moves parallel to the surface and then starts to rise rapidly at a downwind distance $x^* = 0.5$ ($x^* = x w_* / (z_i U_x)$), creating a local maximum of concentration near the inversion layer. This maximum is located at a height of $z = 1.1 z_i$ at about $x^* = 2.0$. This is the same distance downwind as that observed in the laboratory experiments of Willis and Deardorff (1976) ($x^* = 1.75$), but the height is greater ($z = 0.75 z_i$ in the Willis and Deardorff (1976) experiment). This difference between the calculation and the experimental data may be connected to the larger size of the coherent structures in the calculations (see fig. 3, $\lambda_{max}(z)$) near the inversion layer than in the observed data in the ABL. At about $x^* = 2.5$, the centerline begins to descend back into the middle of the ABL in a manner similar to the laboratory results. The plume centerline for the mid-level elevated source descends rapidly, impinging on the ground at $x^* = 0.9$, with a maximum concentration there of $C_y = 1.8 q_0 / (z_i U_x)$ (see fig. 8). Both these features are in good agreement with the experiments (Willis and Deardorff, 1981). The plume then rebounds from the surface, producing a second line of high concentrations, which rises near the inversion layer. The calculated and measured ground-level concentrations for these cases are shown in Fig. 9, 10. The calculated behavior of the plume centerline for both cases corresponds closely the

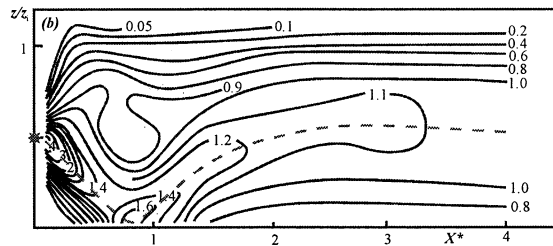
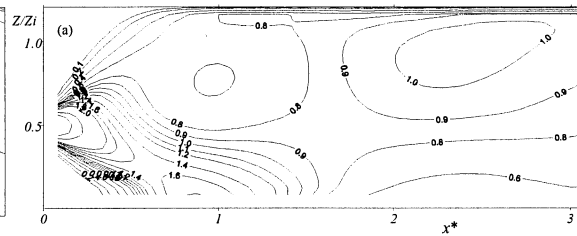


Figure 8. Calculated (a) and measured (Willis and Deardorff, 1981) (b) non-dimensional crosswind integrated concentration for point sources of height $z/z_i = 0.5$.

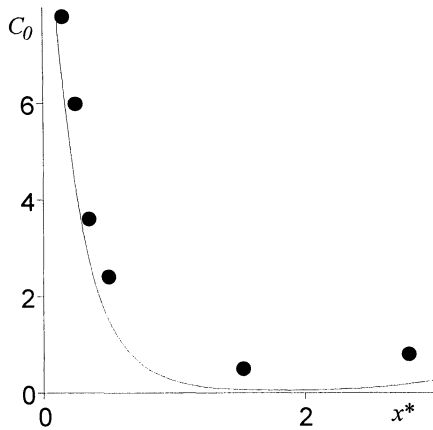


Figure 9. The calculated ground-level concentration (line) compared with the corresponding value from the laboratory experiment (circles) for source height at $0.067 z_i$

Willis and Deardorff's tank experiments. It should be noted that the laboratory experiments did not include wind-shear and Coriolis effects in contrast with the natural ABL observation and the simulation.

To conclude this paper, it should be noted that the accounting of the influence of the coherent structures by separation of the periodic properties of motions is used in VLES. In this paper the approach of accounting the influence of the coherent structures by accentuation of the periodic properties of motions on the PDF level (in contrast with VLES-method) has been presented. This approach can be one of the possible applications of the constructed PDF.

The work was supported by the INTAS (project number 97-2022) and by RFBR (grants N 00-15-96810, 01-01-00783)

REFERENCES

De Baas, A.F., van Dop, H. and Nieuwstadt F.T.M. 1986. "An application of the Langevin equation for inhomogeneous conditions to dispersion in a convective boundary layer". *Quart. J. R. Met. Soc.*, Vol. 112, pp. 165-171.

Byzova N.L., Ivanov V.N., Garger E.K.. 1991. "Experimental investigations of atmospheric diffusion and pollution dispersion calculations". Gidrometeoizdat, Leningrad. (in Russian).

Caughey S.G. 1982. "Observed characteristics of atmospheric boundary layer". In *Atmospheric Turbulence and Air Pollution Modelling* (ed. F.T.M. Nieuwstadt & H. van Dop). D. Reidel, Boston, MA.

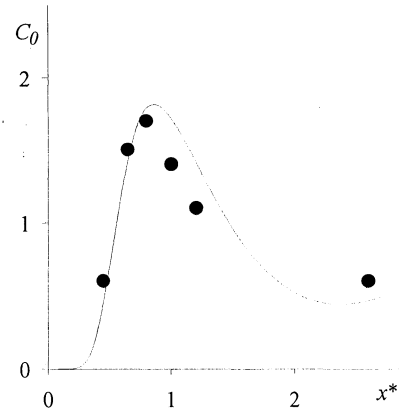


Figure 10. The calculated ground-level concentration for source height at $0.5 z_i$. Line and symbols are as in fig. 9.

Ilyushin B.B., Kurbatskii A.F.. 1996. "Modeling the pollutant spreading in the convective ABL". *Izv. RAN. Phys. Atmos. and Ocean*, Vol. 32, 307-322 (in Russian).

Ilyushin B.B. 1998, "Modelling the non-local turbulent transport of momentum, heat and substance in the convective PBL". *Proc. 2nd International Conference on Turbulent Heat Transfer*, UMIST, Vol. 1, pp. 548-557.

Lenschow D.H., Wyngaard J.C., Pennel W.T. 1980. "Mean-field and second-moment budgets in a baroclinic, convective boundary layer" *J. Atmos. Sci.*, Vol. 37, pp. 1313-1326.

Monin A.S., Yaglom A.M. "Statistical Hydromechanics" (Part 1,2). Moscow: Science, 1967.

Tennekes H., Lumley J.L. 1972. "A First Course in Turbulence. MIT Press, Cambridge, Massachusetts".

Willis, G.E., and J.W. Deardorff. 1976. "A laboratory model of diffusion into the convective boundary layer". *Quart. J. Roy. Meteor. Soc.* Vol. 102, pp. 427-445.

Willis, G.E., and J.W. Deardorff. 1981. "A laboratory study of dispersion from a source in the middle of the convective boundary layer". *Atmos. Environ.* Vol. 15, pp. 109-117.